A Temperature Dependent Lumped-charge Model for Trench FS-IGBT

Duan, Yaoqiang; Kang, Yong; Iannuzzo, Francesco; Trintis, Ionut; Blaabjerg, Frede

Published in:
IEEE Applied Power Electronics Conference and Exposition (APEC), 2018

DOI (link to publication from Publisher):
10.1109/APEC.2018.8341018

Publication date:
2018

A Temperature Dependent Lumped-charge Model for Trench FS-IGBT

Yaoqiang Duan and Yong Kang
School of Electrical and Electronics Engineering
Huazhong University of Science and Technology
Wuhan, China
Email: duanyaoqiang@hust.edu.cn

Francesco Iannuzzo, Ionut Trintis,
and Frede Blaabjerg
Department of Energy Technology
Aalborg University
Aalborg, Denmark
Email: fia@et.aau.dk

***Abstract*—This paper proposes a temperature dependent lumped-charge model for FS-IGBT. Due to the evolution of the IGBT structure, the existing lumped-charge IGBT model established for NPT-IGBT is not suitable for the simulation of FS-IGBT. This paper extends the lumped-charge IGBT model including the field-stop (FS) structure and temperature characteristics. The temperature characteristics of the model are considered for both the bipolar part and unipolar part. In addition, a new PN junction model which can distinguish the collector structure is presented and validated by TCAD simulation. Finally, the lumped-charge FS-IGBT model is implemented in PSPICE and verified by experiments with Infineon FF1000R17IE4 IGBT.**

Keywords—FS-IGBT; Lumped-charge model; PN junction model; Temperature dependent;

I. INTRODUCTION

With the broad application of the IGBT in the converters, a good model which can accurately describe the characteristics of IGBT has been attracting the attention of device manufacturers and circuit designers. However, modeling work of IGBT has never stopped since the fabrication of IGBT in the early 1980s for more than 30 years [1].

Generally, the IGBT models could be classified as behavior model and physical model [2]. Compared with behavior model, physical model can get more accurate simulation results. Besides, physical model based on semiconductor physics could not only model the electrical behavior of device terminals but also give an insight of the carrier transportation inside the device which is very important for the abnormal conditions analysis of IGBT. For now, a lot of physics-based models have been proposed including Hefner model, Kraus model, and the lumped-charge model, etc. [2, 3]. However, the application of these physical models is still limited since it needs to solve physic equations which could result in a time-consuming calculation and extra difficulty for parameter extraction.

Among these physical models, the lumped-charge model represents a good tradeoff between accuracy and simplicity. It based on such a numerical approach where the ambipolar diffusion equation (ADE) is rewritten in a discrete spatial form avoiding the complex numerical solution to ADE. The modeling equations of the lumped-charge model for static and switching characterization have the same form so that it could be easily implemented in circuit simulation platforms, such as PSPICE and SABER. Also, fewer parameters need to be identified in the lumped-charge IGBT model [3].

On the other hand, reliability analysis is getting more and more attention during the design of power electronic system in recent years. The physical models are more suitable to do the failure mechanism study in the circuit simulation. The lumped-charge IGBT model due to the advantages discussed above has been used to do Electrothermal co-simulation of IGBTs under short-circuit condition[4]. But the model utilized in [4] is established for NPT-IGBT and temperature dependent partially. Because the chip structure is different, the NPT-IGBT lumped-charge model couldn't be used to simulate FS-IGBT directly just by parameters adjustment. A new lumped-charge model which can reflect the evolution of IGBT structure and be temperature dependent is of great importance to the power electronic system designers.

The present work in this paper extends the lumped-charge IGBT model in [3], including the field-stop (FS) structure and temperature characteristics. A new PN junction model is proposed for FS-IGBT which could describe the hole injection efficiency of IGBT collector. This PN junction model is validated by TCAD simulation and also suitable for other kinds of IGBT structure. The model parameters extraction procedure is improved and automated through multi-objective optimization algorithms. Finally, the improved lumped-charge model is implemented in PSPICE and verified by experiments with Infineon FF1000R17IE4 IGBT in different temperature and operating conditions.

II. LUMPED-CHARGE MODEL EXTENSION

This section extends and improves the lumped-charge IGBT model in [3]. Firstly, a PN junction model based on collector current is proposed for FS-IGBT. The new model could also describes the hole injection efficiency of IGBT collector and is verified by TCAD simulation.

This work was supported by the National Natural Science Foundation of China under Grant 51490681, by National Key Basic Research Program of China 973 Program under Grant 51507185.

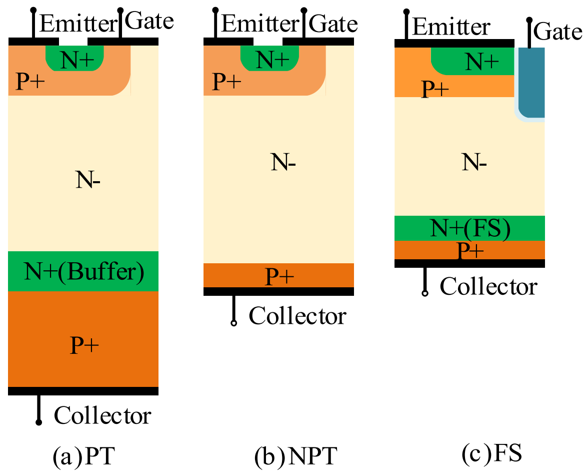

Fig. 1 Evolution of IGBT chip structures

Secondly the modeling methods for bipolar part of IGBT especially for the FS layer are discussed. Then the unipolar part of IGBT was established on the level-3 MOSFET model in PSPICE. Finally, some expressions of the main temperature dependent models in IGBT is given.

A. PN Junction Model in IGBT

PN junction is the basic structure of IGBT. The model of PN junction is relatively simple, but its modeling accuracy will have a significant impact on the injection of holes in the wide base region of IGBT. For the static characteristics, the injection of holes will determine the distribution of carriers in the base region which adjusts the forward voltage drop of IGBT through the conductivity modulation effect. For the turn-off characteristics, the injection of holes will influence the tail current which will be decreased by reducing the holes injection efficiency of the collector. Therefore, optimization of the IGBT collector is always one of the three top development trends of IGBT-based devices [5].

In this paper, the PN junction model is defined as a voltage model and a current model. Voltage model used to describe the relationship of the voltage on PN junction (V_{ji}) and the injection concentration of holes (q_{p2}) shown as follow:

$$\begin{cases} q_{p2} = q_{p20} \cdot \exp(\frac{V_{ji}}{V_T}) & (V_{ji} > 0) \\ q_{p2} = -C_{ji}\big|_{1V} \cdot \sqrt{V_{ji}} & (V_{ji} \le 0) \end{cases} , \quad (1)$$

where $C_{ji}|_{1V}$ is the capacity of the junction between measured at 1V, $q_{p2}= qAd_{FS}p_2$, $q_{p20}= qAd_{FS}p_{20}$. Here q is electron charge; A is the device active area; d_{FS} is the FS region width; p_2 represents the injection concentration of holes under bias condition and p_{20} for hole concentration under thermal equilibrium condition. The quantity q_{p2} is positive when the charge refers to a diffusion condition, and negative when it corresponds to a depletion one. A detailed description of this expression is reported in [3]. Therefore the PN junction model can be expressed as a controlled voltage source. While the lumped-charge IGBT model proposed in [3] only use the voltage model of PN junction and can't tell the difference of different IGBT collector as shown in Fig. 1. Since the different IGBT collector means the different hole injection efficiency from the perspective of modeling. Therefore a current model of PN junction is needed.

The typical current model of PN junction used in the IGBT model comes from the diode model presented in [6]. However, the diode current model was built based on the low-injection condition which the drift current at the PN junction boundary is ignored. For the forward condition of IGBT, especially for large current, the junction works under the condition of high-injection which the drift current couldn't be ignored anymore. Consequently, the diode current model in [6] isn't suitable for IGBT modeling.

In this paper, the current model used to describe the relationship of current go through the PN junction and the injection concentration of holes is induced as follow[7]:

$$I_j = \lambda q A n_i^2 (\frac{q_{p2}}{q_{p20}})(\frac{T}{T_{nom}})^{-1.6}, \quad (2)$$

where λ is the injection coefficient of holes; T is the junction temperature and T_{nom} is the nominal junction temperature. By adjusting the λ, the hole injection efficiency of the PN junction can be changed to accommodate different IGBT collector structures. Under a fixed λ, the quantity of hole injection is determined by the current, and this relationship can be verified by the simulation result of the IGBT turn-on process in TCAD (Fig. 3). In Fig. 3.b, from t_3 to t_6, the current flowing through the IGBT reaches a steady value, the quantity of hole injection to the IGBT collector also reaches a fixed value.

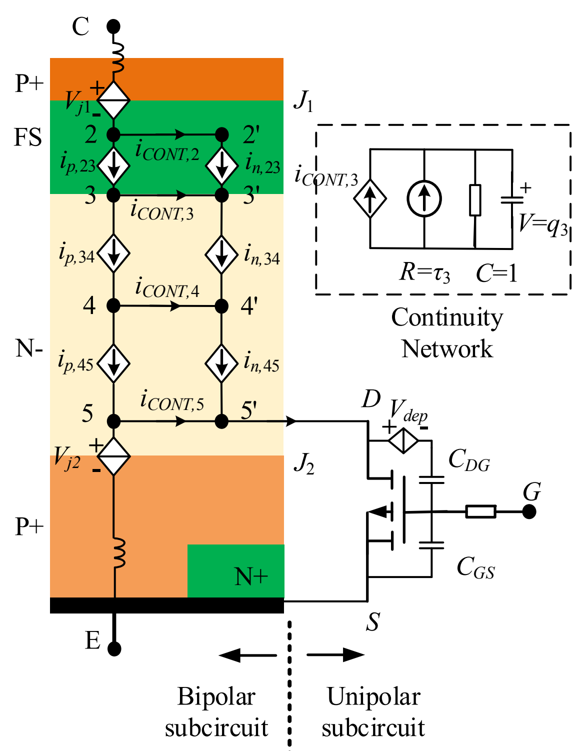

Fig. 2 The lumped-charge model for FS-IGBT

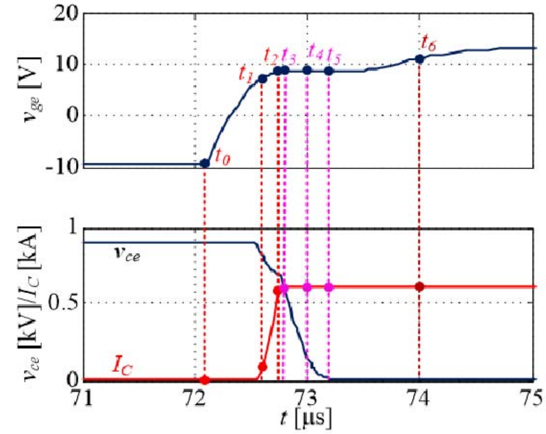

(a)

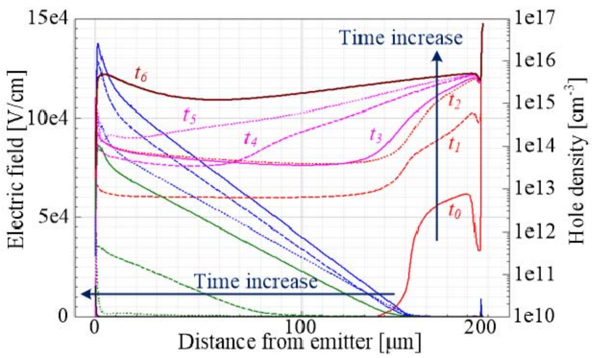

(b)

Fig. 3. TCAD simulation of IGBT turn-on waveforms: (a) Typical IGBT turn-on waveforms with inductive load. (b) Typical hole density and electric field distribution during turn-on process.

B. Bipolar Part Model

As IGBT behaves like a BJT with a MOSFET-controlled base, the lumped-charge IGBT model in this paper is consequently divided into a bipolar (BJT) part and a unipolar (MOSFET) part (Fig. 2).

The bipolar part model of IGBT describes the behavior of the excess carriers injected into the drift region. The typical carrier distribution in the FS-IGBT under the normal forward condition is shown in Fig. 4. As discussed in [8], due to the relatively low-doping concentration of FS layer compared to the P+ collector, the concentration of excess carrier in the FS layer is usually higher than the doping concentration in the N-region. Therefore the assumption of low-injection to the buffer layer [9] is inappropriate to the FS layer. As a result, in this paper, the same high-injection assumption as that for the lightly doped N- region is applied to the FS region

The current model of FS region consists of two types of currents: the currents flowing into and out of the FS layer.

As shown in Fig. 2, the hole current $i_{p,23}$ and the electron current $i_{n,23}$ are the currents following into the FS layer. The gradients of the carrier distribution at the boundary of the FS layer, which can be expressed as a function of $i_{p,23}$ and $i_{n,23}$

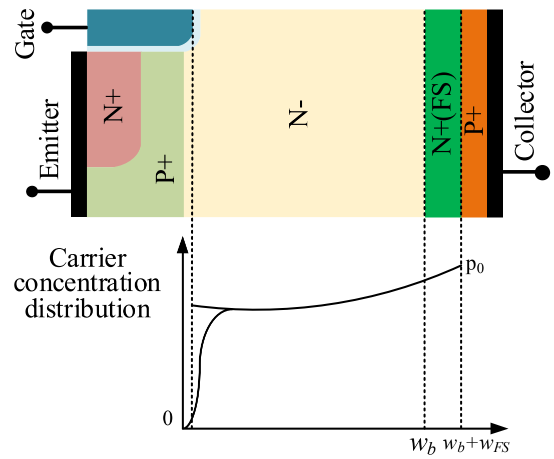

Fig. 4 Typical carrier distribution in the FS-IGBT under forward condition

$$\left.\frac{\partial p}{\partial x}\right|_2 = \frac{1}{2qA}\left(\frac{i_{n,23}}{D_{Fn}} - \frac{i_{p,23}}{D_{Fp}}\right), \tag{3}$$

where D_{Fn} is electron diffusion coefficient, and D_{Fp} is hole diffusion coefficient in the FS region.

According to the current density equation, the hole current $i_{p,23}$ and the electron current $i_{n,23}$ are defined as

$$\begin{cases} i_{p,23} = q\dfrac{D_{Fp}}{V_T}p_2AE - qD_{Fp}A\left.\dfrac{\partial p}{\partial x}\right|_2 \\ i_{n,23} = q\dfrac{D_{Fn}}{V_T}p_2AE + qD_{Fn}A\left.\dfrac{\partial p}{\partial x}\right|_2 \end{cases}, \tag{4}$$

The relationship between the adjacent lumped-charge could be expressed as a current generator in the circuit simulation platform(Fig. 2). Substitut (3) into (4), the Lumped-charge form of $i_{p,23}$ and $i_{n,23}$ could be given by

$$\begin{cases} i_{p,23} = \dfrac{q_{p2}}{T_{p23}}\dfrac{V_{23}}{V_T} - \dfrac{D_{Fp}}{D_{Fn}-D_{Fp}}I_j \\ i_{n,23} = \dfrac{q_{p2}}{T_{n23}}\dfrac{V_{23}}{V_T} + \dfrac{D_{Fn}}{D_{Fn}-D_{Fp}}I_j \end{cases}, \tag{5}$$

where $T_{p12} = \dfrac{d_{FS}^2\cdot\left(D_{Fn}-D_{Fp}\right)}{2D_{Fp}D_{Fn}}$, and $T_{n12} = -\dfrac{d_{FS}^2\cdot\left(D_{Fn}-D_{Fp}\right)}{2D_{Fp}D_{Fn}}$.

See Fig. 2, the hole current $i_{p,34}$ and the electron current $i_{n,34}$ are the currents following out of the FS layer and they can be expressed as

$$\begin{cases} I_{p,34} = q\dfrac{D_{Fp}}{V_T}p_3AE + qAD_{Fp}\dfrac{p_2-p_3}{d_{FS}} \\ I_{n,34} = q\dfrac{D_{Fn}}{V_T}(p_3+N_{FS})AE - qAD_{Fn}\dfrac{p_2-p_3}{d_{FS}} \end{cases}. \tag{6}$$

N_{FS} is the background doping concentration in the FS region, and p3 is the hole concentration at the boundary of the

FS region and N- base region. Transform (6) into the lumped-charge form as

$$\begin{cases} I_{p,34} = \dfrac{q_{p2}}{T_{p34}}\dfrac{V_{34}}{V_T} + \dfrac{q_{p2}-q_{p3}}{\tilde{T}_{p34}} \\ I_{n,34} = \dfrac{q_{p2}+q_{FS}}{T_{n34}}\dfrac{V_{34}}{V_T} + \dfrac{q_{p2}-q_{p3}}{\tilde{T}_{n34}} \end{cases}, \quad (7)$$

where $T_{p34} = \dfrac{d_B^2}{D_{Fp}}, \tilde{T}_{p34} = \dfrac{d_{FS}\cdot d_B}{D_{Fp}}$.

$$T_{n34} = \dfrac{d_B^2}{D_{Fn}}, \tilde{T}_{n34} = \dfrac{d_{FS}\cdot d_B}{D_{Fn}}.$$

$q_{p2} = qp_2 Ad_B$ and $q_{p3} = qp_3 Ad_B$. d_B is the base region width.

The currents flowing through the horizontal branches placed in Fig.2 between nodes 2-2', etc. represent the recombination current of the adjacent lumped-charge. These recombination currents must satisfy the continuity equation in the following (e.g., 2-2'):

$$i_{CONT,2} = i_{p,23} - i_{p,34} = \frac{dq_{p2}}{dt} + \frac{q_{p2}}{\tau_{FS}}, \quad (8)$$

where τ_{FS} is the hole carrier lifetime in FS layer.

In conclusion, here all the equations for the modeling of FS region are given by (5), (7) and (8). The detail modeling method of N- base region of IGBT could be found in [3].

C. *Unipolar Part Model*

As shown in Fig. 2, an advanced MOSFET model has been included to describe the unipolar structure of FS-IGBT. The unipolar part model consists of a PSPICE level-3 MOSFET model and a series voltage controlled generator on the capacitance C_{GD} to present the nonlinear behavior of the capacitance in depletion conditions [3]. The source of MOSFET is connected to the emitter, and the drain to the node 5' to reproduce the electron injection in the drift region.

The static characteristics of the level-3 MOSFET model is determined by a controlled current source to present the channel current using the Shockley equations

$$I_{MOS} = \begin{cases} 0 & (V_{gs} - V_{th}) \\ K_p[(V_{gs} - V_{th})V_{ds} - \frac{1}{2}V_{ds}^2] & (V_{gs} - V_{th} \geq V_{ds}) \\ \dfrac{K_p}{2}(V_{gs} - V_{th})^2 & (V_{gs} - V_{th} < V_{ds}) \end{cases}, \quad (9)$$

where I_{MOS} is the channel current; K_P is transconductance parameter; V_{gs} is intrinsic gate–source voltage, and V_{th} is channel threshold voltage.

The voltage generator V_{dep} (Fig. 2) is determined by a controlled voltage source defined as

$$V_{dep} = \begin{cases} V_{dg} + V_n(1 - \sqrt{1 + \dfrac{2V_{dg}}{V_n}}) \\ 0 \end{cases}. \quad (10)$$

V_{dg} is intrinsic gate–drain voltage, and V_n is a normalization factor mainly dependent on the gate–drain overlap area and doping of base region.

D. *Other Temperature Dependent models*

The characteristics of IGBT have a strong correlation with temperature[1]. Therefore the model of IGBT should not only describe the electrical behavior but also give a characterization of temperature properties. The main temperature dependent models of IGBT are given as follow.

a) Electron and Hole mobility: the mobility of carriers related to temperature and doping concentration, the model of them defined as[10]

$$\mu_p = 54.3\cdot(\frac{T}{300})^{-0.57} + \frac{407\cdot(\frac{T}{300})^{-2.33}}{(1+\dfrac{N_B}{2.35\times10^{17}\cdot(\frac{T}{300})^{2.4}})^{\alpha}}, \quad (11)$$

$$\mu_n = 88\cdot(\frac{T}{300})^{-0.57} + \frac{1252\cdot(\frac{T}{300})^{-2.33}}{(1+\dfrac{N_B}{1.26\times10^{17}\cdot(\frac{T}{300})^{2.4}})^{\alpha}}. \quad (12)$$

$\alpha=0.88(T/300)^{-0.146}$. μ_p is the hole mobility and μ_n is the electron mobility.

b) Carrier lifetime: Carrier lifetime is not only related to temperature and doping concentration but also to carrier injection level. The hole lifetime in FS region τ_{FS} and base region τ_B is given by[8]

$$\tau_{FS}(T) = \tau_{FS}(T_{nom})(T/T_{nom})^{1.5}, \quad (13)$$

$$\tau_B(T) = \tau_B(T_{nom})(T/T_{nom})^{1.7}. \quad (14)$$

c) Transconductance parameter: the forward voltage drop in MOS channel is decided by K_p.

$$K_P(T) = K_P(T_{nom})(T/T_{nom})^{-0.8}. \quad (15)$$

d) Channel threshold voltage:

$$V_{th}(T) = V_{th}(T_{nom}) - 9\times10^{-3}(T - T_{nom}). \quad (16)$$

III. PARAMETER EXTRACTION AND OPTIMIZATION

Physics-based model of IGBT gives a better insight of the complex failure mechanisms as well as a good prediction of IGBT static and transient characteristics for circuit designers.

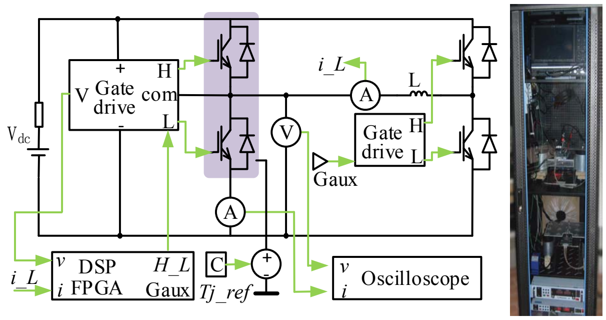

Fig. 5 The triple pulse test setup for IGBT

However, the use of it has been accompanied by some challenges which one of them is the model parameters extraction [11].

In this paper, the parameters extraction of the lumped-charge model comprises two steps. The first step is the evaluation of the parameters including device structural parameters and circuit parasitic parameters. These parameters are not easily accessible without reverse engineering facilities or the data provided by the device manufacturers. However, in the development of physics-based models, with the improvement of experimental conditions, some literatures have proposed a series of model parameters extraction methods [2]. These methods could be used to estimate the parameters preliminarily.

Then, the second step is using the software MBPI(Model Based Parameter Identifier) presented in [11] to do the optimization of parameters extracted in the first step. Through the optimization, the accuracy of the physical model will be further improved.

IV. Model Implementation And Experimental Verification

The lumped-charge FS-IGBT model discussed in the previous sections has been transferred in the form of an equivalent circuit and can be implemented in circuit simulator (Fig. 2). In this paper, we develop the lumped-charge model in the PSPICE simulator with a user-defined device library.

In order to compare with the simulation results, a commercially available IGBT module, Infineon FF1000R17IE4, has been tested with the IGBT triple pulse test setup designed in [12] (Fig. 5). The test platform can accurately characterize the switching of IGBT with different bus voltage and load current.

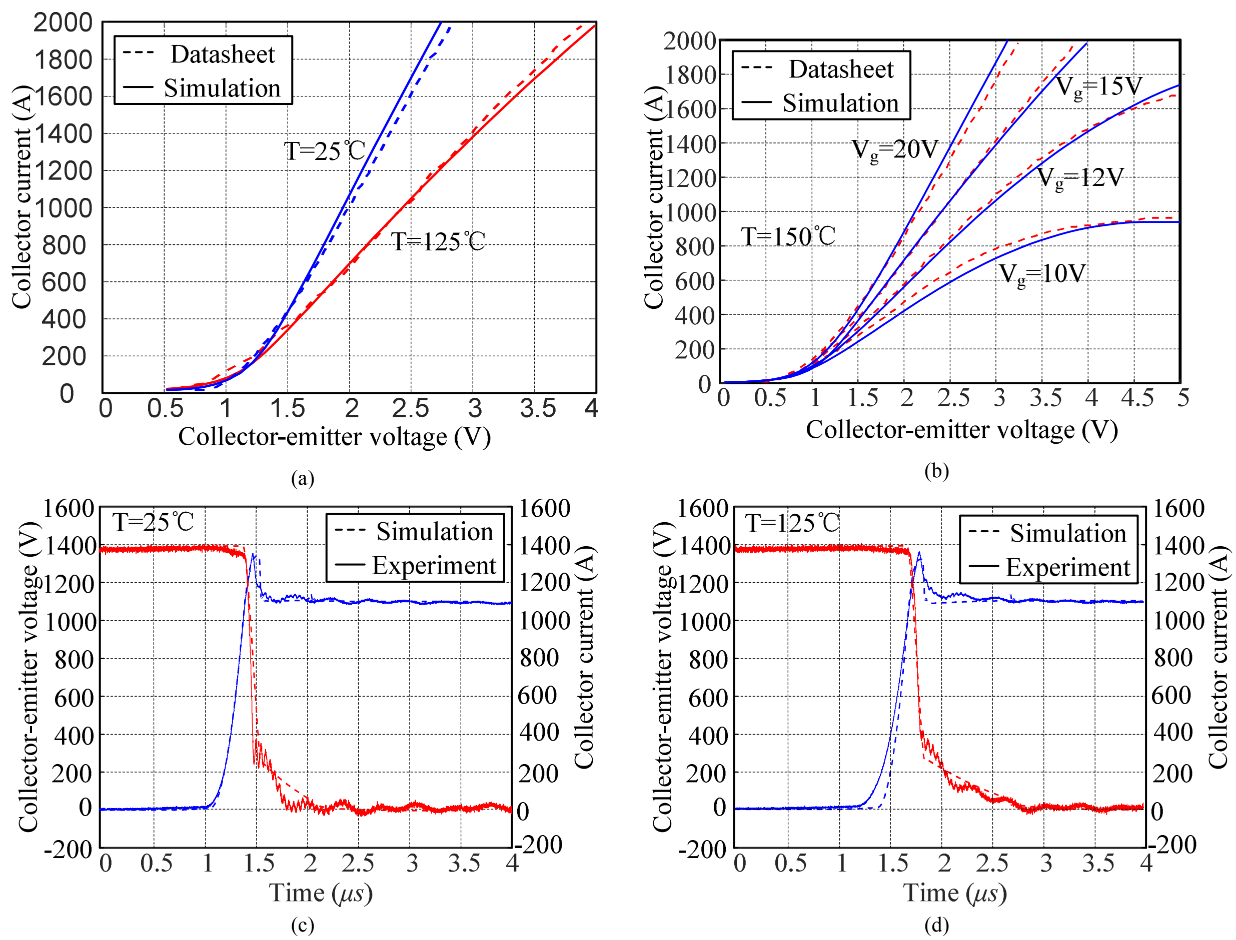

Fig. 6 Comparison between experiment and simulation waveforms: (a) Static characteristics of IGBT at 25℃ and 125℃. (b) Static characteristics of IGBT under different gate voltage. (c) Turn-off waveforms with chip temperature at 25℃. (d) Turn-off waveforms with chip temperature at 125℃.

Besides, the temperature of the IGBT chip could also be set by a temperature control loop. Fig.6 illustrates the comparison between experimental results and simulation waveforms.

As shown in Fig. 6, the proposed model obtains accurate simulation results both for the FS-IGBT static and transient characteristics, especially for tail current at different temperature conditions.

V. Conclusions

This paper develops a temperature dependent lumped-charge model for FS-IGBT. Firstly, a PN junction model based on collector current which can distinguish the collector structure of IGBT is presented and validated by TCAD simulation. The major contribution of this paper is the establishment of lumped-charge expressions for FS layer of IGBT. The accuracy of the FS-IGBT model has been verified by an Infineon FF1000R17IE4 IGBT, proving that the proposed model accurately describes the static and dynamic behavior of FS-IGBT at different temperature and load conditions.

Acknowledgment

The authors gratefully acknowledge the financial support from China Scholarship Council (CSC).

References

[1] B. J. Baliga, The IGBT device: Physics, design and applications of the insulated gate bipolar transistor: William Andrew, 2015, pp.1–17.

[2] S. Kuang, B. W. Williams, and S. J. Finney, "A review of IGBT models," IEEE Trans. Power Electron., vol. 15, no. 6, pp. 1250-1266, Nov. 2000.

[3] F. Iannuzzo and G. Busatto, "Physical cad model for high-voltage IGBTs based on lumped-charge approach," IEEE Trans. Power Electron., vol. 19, no. 4, pp. 885-893, Jul. 2004.

[4] R. Wu, F. Iannuzzo, H. Wang, and F. Blaabjerg, "Fast and accurate Icepak-PSpice co-simulation of IGBTs under short-circuit with an advanced PSpice model," in 7th IET Int. Conf. Power Electron., Machines and Drives, Apr. 2014, pp. 1-5.

[5] A. Kopta, M. Rahimo, C. Corvasce, M. Andenna, F. Dugal, F. Fischer, S. Hartmann, and A. Baschnagel, "Next generation IGBT and package technologies for high voltage applications," IEEE Trans. Electron Devices, vol. 64, no. 3, pp. 753-759, Mar. 2017.

[6] S. Ji, Z. Zhao, T. Lu, L. Yuan, and H. Yu, "Hvigbt physical model analysis during transient," IEEE Trans. Power Electron., vol. 28, no. 5, pp. 2616-2624, May. 2013.

[7] S. E. Fred, Led basics: Electrical in light-emitting diode: Cambridge, 2006, pp.59-61.

[8] Y. Chen, H. Luo, W. Li, X. He, F. Iannuzzo, and F. Blaabjerg, "Analytical and experimental investigation on a dynamic thermo-sensitive electrical parameter with maximum dIc/dt during turn-off for high power trench gate/field-stop IGBT modules," IEEE Trans. Power Electron., vol. 32, no. 8, pp. 6394-6404, Aug. 2017.

[9] S. Ji, T. Lu, Z. Zhao, T. Fujihira, and S. Igarashi, "Physical model with parameter extraction method for Fuji electric 1.7kV IGBT," in 18th Int. Conf. Electrical Machines and Systems Oct. 2015, pp. 587-590.

[10] MEDICI User's Manual, Avant! Corporation, Palo Alto, CA, 1998.

[11] C. G. Suarez, P. D. Reigosa, F. Iannuzzo, I. Trintis, and F. Blaabjerg, "Parameter extraction for PSpice models by means of an automated optimization tool - an IGBT model study case," in PCIM Europe 2016; International Exhibition and Conference for Power Electronics, Intelligent Motion, Renewable Energy and Energy Management, 10-12 May 2016 2016, pp. 1-8.

[12] I. Trintis, T. Poulsen, S. Beczkowski, S. Munk-Nielsen, and B. Rannestad, "Triple pulse tester-efficient power loss characterization of power modules," in 17th European Conference on Power Electronics and Applications, Sept. 2015, pp. 1-7.